AGU PUBLICATIONS

JGR

Journal of Geophysical Research: Oceans

RESEARCH ARTICLE

10.1002/2017JC013094

How are warm and cool years in the California Current related to ENSO?

Paul C. Fiedler[1] **and Nathan J. Mantua**[2]

[1]Marine Mammal and Turtle Division, Southwest Fisheries Science Center, National Marine Fisheries Service, National Oceanic and Atmospheric Administration, La Jolla, California, USA, [2]Fisheries Ecology Division, Southwest Fisheries Science Center, National Marine Fisheries Service, National Oceanic and Atmospheric Administration, Santa Cruz, California, USA

Key Points:
- California Current System (CCS) warm/cool events do not always co-occur with tropical ENSO events, and vice versa
- Local wind forcing is correlated with SST anomalies in most of the CCS, but remote tropical forcing is most important in the south
- CCS warm/cool events are more intense when there is a concurrent ENSO event

Correspondence to:
P. Fiedler,
paul.fiedler@noaa.gov

Citation:
Fiedler, P. C., and N. J. Mantua (2017), How are warm and cool years in the California Current related to ENSO?, *J. Geophys. Res. Oceans*, *122*, 5936–5951, doi:10.1002/2017JC013094.

Received 12 MAY 2017
Accepted 26 JUN 2017
Accepted article online 5 JUL 2017
Published online 27 JUL 2017

Abstract The tropical El Niño-Southern Oscillation (ENSO) is a dominant mode of interannual variability that impacts climate throughout the Pacific. The California Current System (CCS) in the northeast Pacific warms and cools from year to year, with or without a corresponding tropical El Niño or La Niña event. We update the record of warm and cool events in the CCS for 1950–2016 and use composite sea level pressure (SLP) and surface wind anomalies to explore the atmospheric forcing mechanisms associated with tropical and CCS warm and cold events. CCS warm events are associated with negative SLP anomalies in the NE Pacific—a strong and southeastward displacement of the wintertime Aleutian Low, a weak North Pacific High, and a regional pattern of cyclonic wind anomalies that are poleward over the CCS. We use a first-order autoregressive model to show that regional North Pacific forcing is predominant in SST variations throughout most of the CCS, while remote tropical forcing is more important in the far southern portion of the CCS. In our analysis, cool events in the CCS tend to be more closely associated with tropical La Niña than are warm events in the CCS with tropical El Niño; the forcing of co-occurring cool events is analogous, but nearly opposite, to that of warm events.

Plain Language Summary The California Current System in the northeast Pacific warms and cools from year to year, with or without a corresponding tropical El Niño or La Niña event. We update the record of warm and cool events in the California Current for 1950-2016 and use sea level pressure and surface wind data to explore the atmospheric forcing of these events. California Current warm events are associated with a strong and southeastward displacement of the wintertime Aleutian Low, a weak North Pacific High and a regional pattern of poleward coastal wind anomalies. Regional North Pacific forcing is predominant in sea surface temperature variations throughout most of the California Current, while remote tropical forcing is more important in the far southern portion. In our analysis, local cool events tend to be more closely associated with tropical La Niña than are warm events with El Niño; the forcing of co-occurring cool events is analogous, but nearly opposite, to that of warm events. Understanding variations between years in the California Current may help predict and manage changes in fisheries and climate of the region.

1. Introduction

Variability of the ocean, both regionally and globally, and ecosystem consequences have garnered much attention due to concern about climate change and events such as El Niño and the recent marine heat-waves in Western Australia, the Northwest Atlantic, and the Northeast Pacific [*Scannell et al*., 2016; *Hobday et al*., 2016; *DiLorenzo and Mantua*, 2016]. The El Niño-Southern Oscillation (ENSO) is a dominant mode of interannual climate variability with maximum amplitude in the tropical Pacific [*McPhaden et al*., 2006]. ENSO has global climate effects through oceanic and atmospheric teleconnections [*Liu and Alexander*, 2007]. Regional patterns of interannual variability occur everywhere in the ocean; year-to-year differences are the rule even at higher latitudes where seasonality in solar forcing modulates ocean-atmosphere exchanges of heat, water, and momentum. Interannual variations in atmospheric circulation affect sea surface temperature (SST), or the temperature of the upper-ocean mixed layer, by the exchange of energy at the sea surface and by heat transport through currents and vertical mixing [*Deser et al*., 2010].

A gathering of pragmatic oceanographers and meteorologists in 1959, for a CalCOFI "Symposium on the Changing Pacific Ocean in 1957 and 1958," compiled observations on physical and biological changes throughout the Pacific [*Sette and Isaacs*, 1960]. Many of these widespread effects were due in part to the tropical Pacific El Niño and coincident prolonged warming in the California Current System (CCS) that had begun in 1957. They summarized "that locally observed changes in ocean conditions, marine fauna, fisheries success, weather, etc., are often the demonstrable result of processes acting over vast areas." Although they realized that interactions between the atmosphere and ocean must be involved, causal mechanisms were not elaborated at the time. It was a decade later that *Bjerknes* [1969] published the first description of ENSO as a phenomenon involving ocean-atmosphere feedback across the entire tropical Pacific, including effects at higher latitudes.

Interannual variability of monthly SST anomalies in the CCS (CCSTA) and the equatorial Pacific (NINO34, a widely used index for ENSO [*Trenberth*, 1997]) are similar in amplitude and phase (Figure 1); correlation of the monthly time series is maximum at 0.53, when CCSTA lags NINO34 by 1 month. We use October–March mean CCSTA and NINO34 to remove the influence of subseasonal lags and autocorrelation. The correlation between the October–March mean time series is 0.65, such that only 42% of the interannual variance of SST in the California Current is shared with ENSO. Obvious matches or mismatches of warm events in the two regions are apparent in Figure 1. For example, the record-breaking 1997–1998 El Niño coincided with a 1.5°C warming of the CCS. On the other hand, the CCS was not anomalously warm during the 1986–1987 El Niño, while the CCS was warm in 1995–1996 when NINO34 was cold.

Following the major 1982–1983 El Niño, *Simpson* [1984], *Emery and Hamilton* [1985], and *Mysak* [1986] all recognized the association of NE Pacific warm events and ENSO. Mysak explicitly noted that not all tropical El Niño events have an effect at higher latitudes, and that local atmospheric anomalies can force changes along the North American coast in years with no tropical El Niño. Simpson argued that, during the 1982–1983 El Niño, anomalous atmospheric forcing in the northeast Pacific modulated the normal seasonal cycle resulting in warming and other changes in the CCS.

Recent studies using regional ocean circulation models have provided more insights into the relative importance of regional atmospheric versus remote ocean forcing on the seasonal and interannual variability in the CCS. *Frischknecht et al.* [2015] showed that a Pacific basin-scale ocean circulation model under historical atmospheric forcing reproduces many of the observed features of CCS and ENSO physical variability. They found that remote forcing via oceanic internal wave processes dominates the variability of the physical state in the nearshore region (within 50 km of the coast) of the CCS, accounting for up to 80% of the simulated variability in sea surface height and mixed-layer temperature from 1979 to 2013, while local wind

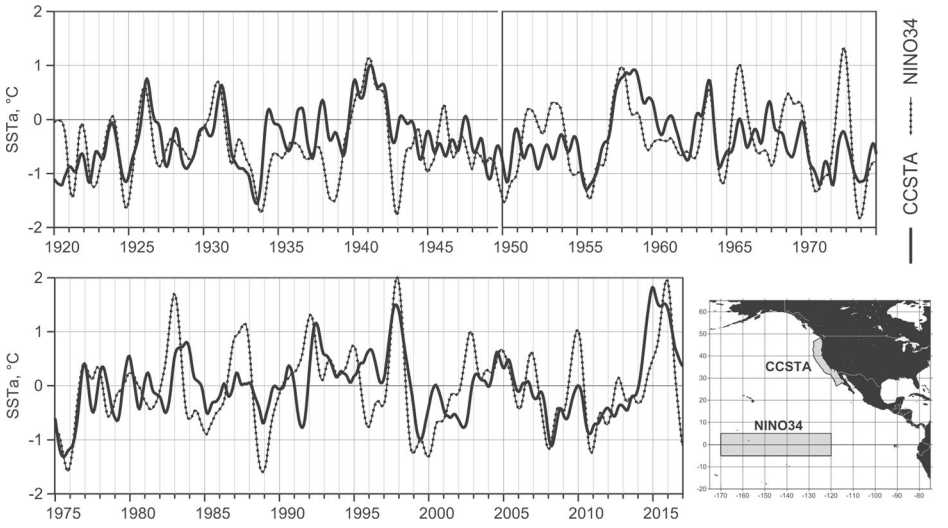

Figure 1. Monthly SST anomalies 1920–2016, 12 month lowess smoothed, in two regions indicated in the inset: the California Current (CCSTA) and the tropical Pacific (NINO34, the NINO3.4 ENSO index region). Data are from NOAA/CDC ERSST V4; anomalies calculated from 1981 to 2010 monthly means.

forcing dominated the simulated biogeochemical variations in the CCS. They also found that local forcing was most important at higher latitudes of the CCS, while remote forcing was most important at lower latitudes of the CCS. *Jacox et al.* [2015a] used an atmospherically forced regional ocean circulation model and found that local wind forcing accounted for most of a simulated trend in nitrate fluxes in the nearshore CCS from 1980 to 2010, while ENSO-related interannual variations were driven equally by local winds and remote forcing.

This new look at California Current and tropical (El Niño) warm events was prompted by the extreme warming of surface waters in the northeast Pacific that began in winter 2013–2014, dubbed "the Blob" [*Bond et al.*, 2015] and described as a marine heatwave [*DiLorenzo and Mantua*, 2016], and the ensuing major El Niño that peaked in winter 2015–2016. We examine regional interannual variations of SST and SLP from 1950 to 2016 and examine these time series for correlations consistent with atmospheric forcing of CCSTA. We use a multivariate analysis of SST and SLP variations to objectively classify annual CCS and ENSO events in a simple matrix of warm, cool, and co-occurrence categories. We examine corresponding temporal and spatial composites of SLP and surface winds to look for differential patterns that might remotely or locally force CCSTA variations. We also show that the atmospheric forcing of co-occurring CCS cool events and tropical La Niñas is consistent with (and essentially opposite) the forcing of co-occurring CCS warm events and tropical El Niños. This analysis focuses on warm/cool events of 1–2 year duration; we are not addressing longer scale (decadal) warm/cold regimes or century-scale warming trends.

2. Materials and Methods

2.1. Data Sources

Monthly SSTs were obtained from the NOAA Climate Data Center Extended Reconstructed Sea Surface Temperature (ERSST) V4 data set (ftp.cdc.noaa.gov/Datasets/noaa.ersst/, accessed 6 January 2017) [*Huang et al.*, 2015]. We used the NINO3.4 index for SST anomalies associated with ENSO (5°S–5°N, 170°W–120°W; NINO34 in Figure 1). California Current SST was indexed by the mean monthly SST anomaly within 300 km of the coast between Cape Flattery at 48.4°N and Punta Eugenia at 27.9°N (CCSTA).

Monthly sea level pressure (SLP) and surface wind velocities were obtained from the NCEP/NCAR Reanalysis data set (ftp.cdc.noaa.gov/Datasets/ncep.reanalysis.derived/, accessed 2 February 2017) [*Kistler et al.*, 2001]. Winter (October–March) and summer (April–September) climatologies of SLP and surface wind velocities are shown in Figure 2. We used composites of (October–March) SLP for warm and cold events in the CCS to identify the regional patterns of SLP anomalies typically associated with interannual variations in CCS SST. Based on the region with maximum SLPa correlation with CCSTA, a monthly Northeast Pacific SLPa index (NEP) was calculated by areally averaging monthly SLP anomalies in the region 120°W–170°W, 30°N–50°N (Figure 3). This region lies between the climatological positions of the wintertime Aleutian Low and North Pacific High pressure centers and substantially overlaps the climatological position of the North Pacific High in summer; we interpret this index as tracking variability in both of these systems. Monthly equatorial

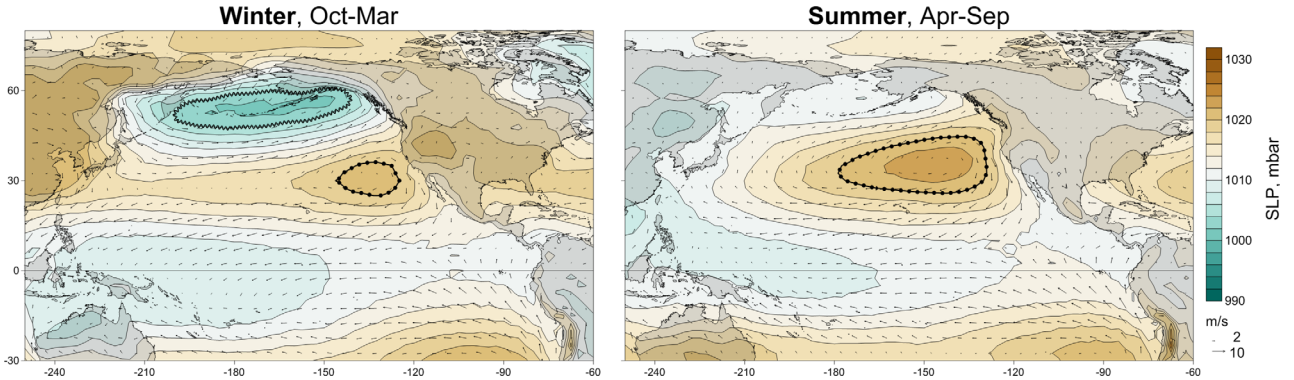

Figure 2. Seasonal climatologies of SLP and surface winds, 1981–2010. The Aleutian Low is the blue center in the winter far North Pacific. The North Pacific High is the brown center in the eastern North Pacific, stronger in summer. The 1004 mbar (wavy line) and 1020 mbar (dotted line) isobars mark the climatological positions of these pressure centers in Figures 8 and 11.

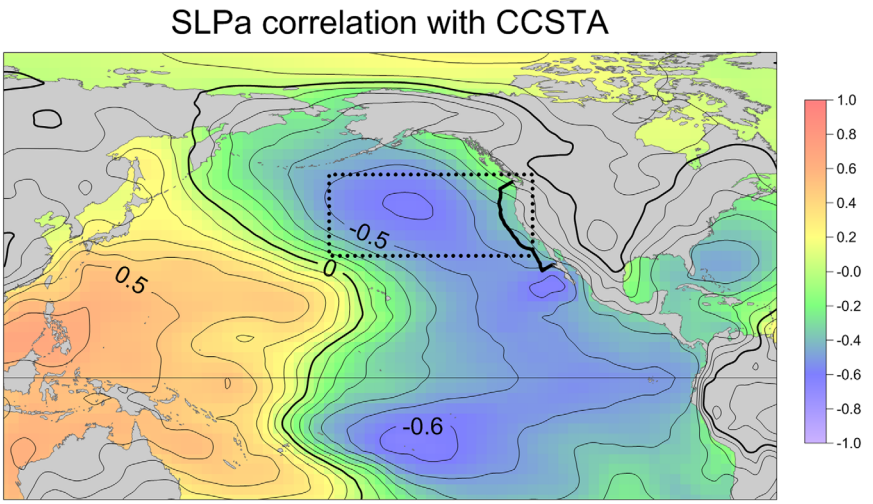

Figure 3. Correlation of yearly October–March SLPa with California Current SSTa (CCSTA region marked with bold line), during 1950–2015. The dotted line is the box for the NEP regional SLPa index.

Southern Oscillation Index (EqSOI) data were obtained from NOAA/NWS/CPC (http://www.cpc.ncep.noaa.gov/data/indices/). EqSOI is an index of ENSO variability of the equatorial SLP gradient across the Pacific and the associated forcing of equatorial Kelvin waves and the coastally trapped waves excited along the eastern boundary of the Pacific Ocean [*Li and Clarke*, 1994].

To identify interannual scale events, the January 1950 to December 2016 time series of SSTa was first high-pass filtered by subtracting the 20 year lowess-smoothed monthly anomalies, and then standardized by dividing by the standard deviation (CCSTA and NINO34, respectively). The time series of SLPa variables were treated in the same way to give standardized NEP and EqSOI.

2.2. Compositing and Regression Analysis

Identification of El Niño and CCS warm/cool events, when the events did or did not co-occur, was done using a principal components analysis (PCA) of yearly winter (October–March) means of both SSTa (CCSTA and NINO34) and SLPa (NEP and EqSOI) variables. In general, years identified as warm or cool events had standardized SSTa values $>+1$ or <-1 for five or more consecutive months, although this period was not always confined to October–March. Some years that followed a year with similar SSTa values, and thus PC scores, were excluded. 2014–2016 were not included in composites because of the unique nature of the North Pacific and El Niño warm events during this period (see section 4).

We fit a linear, first-order, autoregressive model for monthly, gridded ERSST in the NE Pacific using the observed high-pass filtered NEP SLPa and the EqSOI as forcings from 1950 to 2014:

$$\text{Model 1}: \quad T_t - a * T_{t-1} = b_1 * \text{NEP}_t + \varepsilon_t \tag{1}$$

$$\text{Model 2}: \quad T_t - a * T_{t-1} = b_2 * \text{EqSOI}_t + \varepsilon_t \tag{2}$$

where a is the lag-1 autocorrelation of the high-pass filtered SSTa time series at each grid point, b_1 is the linear regression coefficient between the monthly high-pass filtered NEP SLPa and the gridded autoregression residual SSTa, b_2 is the linear regression coefficient between the monthly high-pass filtered EqSOI SLPa and the gridded autoregression residual SSTa, and ε_t is a residual error (unique for each grid cell).

3. Results

We examined correlations among the October–March yearly means (1950–2015) of the two monthly regional surface temperature indices (CCSTA and NINO34) and the two corresponding forcing variables, the atmospheric surface pressure anomaly indices for the northeast Pacific (NEP) and the tropical Pacific (EqSOI). Averaging over 6-month winter seasons reduces noise in the monthly atmospheric series to focus on the integrated response of the ocean to atmospheric forcing. The lag-1 autocorrelation of monthly SSTa

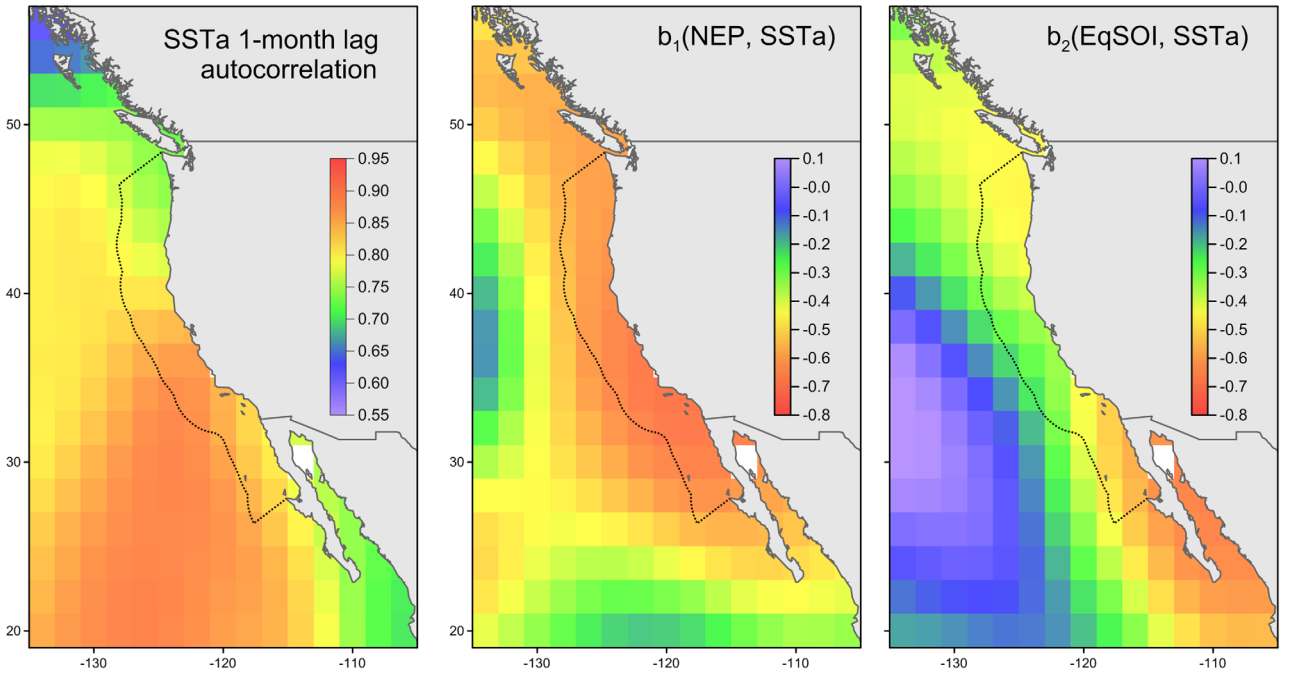

Figure 4. (left) Lag-1 autocorrelation of monthly SSTa, 1950–2016. (center) Regression coefficients of October–March high-pass filtered gridded SSTa (1950–2015) based on equation (1) for NEP forcing and (right) equation (2) for EqSOI forcing. Dotted line is the boundary for areal mean CCSTA.

(Figure 4, left) shows larger values in the central and southern CCS (∼0.85) that extend offshore of Baja California, and the smallest values at the northern end of the CCS (∼0.70). EqSOI and NINO34 are strongly correlated (−0.96, Table 1), as expected. As a result, the correlations of CCSTA with NINO34 and EqSOI are nearly equivalent (+0.66 and −0.65). The correlation between the two atmospheric forcing variables, NEP and EqSOI, is somewhat weaker at +0.58, but this correlation reflects a teleconnection that influences the covariation of CCSTA and NINO34. The correlation of CCSTA with NEP (−0.65) is much weaker than the ocean-atmosphere correlation in the tropics, but still statistically significant.

The spatial patterns for NEP regressions (b_1, equation (1)) are consistent with local forcing: regression coefficients are maximum in the center of the CCS (Figure 4, center). In contrast, the patterns for EqSOI regressions (b_2, equation (2)) are consistent with an especially clear signature of remote forcing from the tropics: regression coefficients are highest along the coast with maximum values off Baja California and decreasing (becoming less negative) poleward (Figure 4, right). A secondary local maximum in b_2 at the northern end of the CCS is consistent with the ENSO-driven atmospheric teleconnection that results in the ENSO-related local forcing of SST variations in the NE Pacific.

3.1. Categorization of Events

Results of the PCA of the two surface temperature (CCSTA and NINO34) and corresponding atmospheric forcing variables (NEP and EqSOI) are summarized in Figure 5. The first two principal components account for more than 90% of the ocean-atmosphere variability described by these four time series. PC1 explains 77.4% and captures in-phase warming and cooling in both regions. Thus, winters with concurrent warm or cool events lie at the extremes of the horizontal (PC1) axis. The variable loading vectors reflect the associations of warm CCSTA with low NEP (strong Aleutian Low and weak North Pacific High) and of warm NINO34 with low EqSOI (weak equatorial SLP gradient between the Indonesian Low and SE Pacific High). PC2 captures an additional 12.9% of the variability and separates California Current from tropical variables, i.e., it captures variability in the two regions that either is out of

Table 1. Correlations of October–March Regional SSTa (CCSTA and NINO34) and SLPa (NEP and EqSOI), 1950–2016[a]

	NINO34	NEP	EqSOI
CCSTA	+0.65	−0.64	−0.65
NINO34		−0.57	−0.96
NEP			+0.58

[a]All $P < 1e{-}7$.

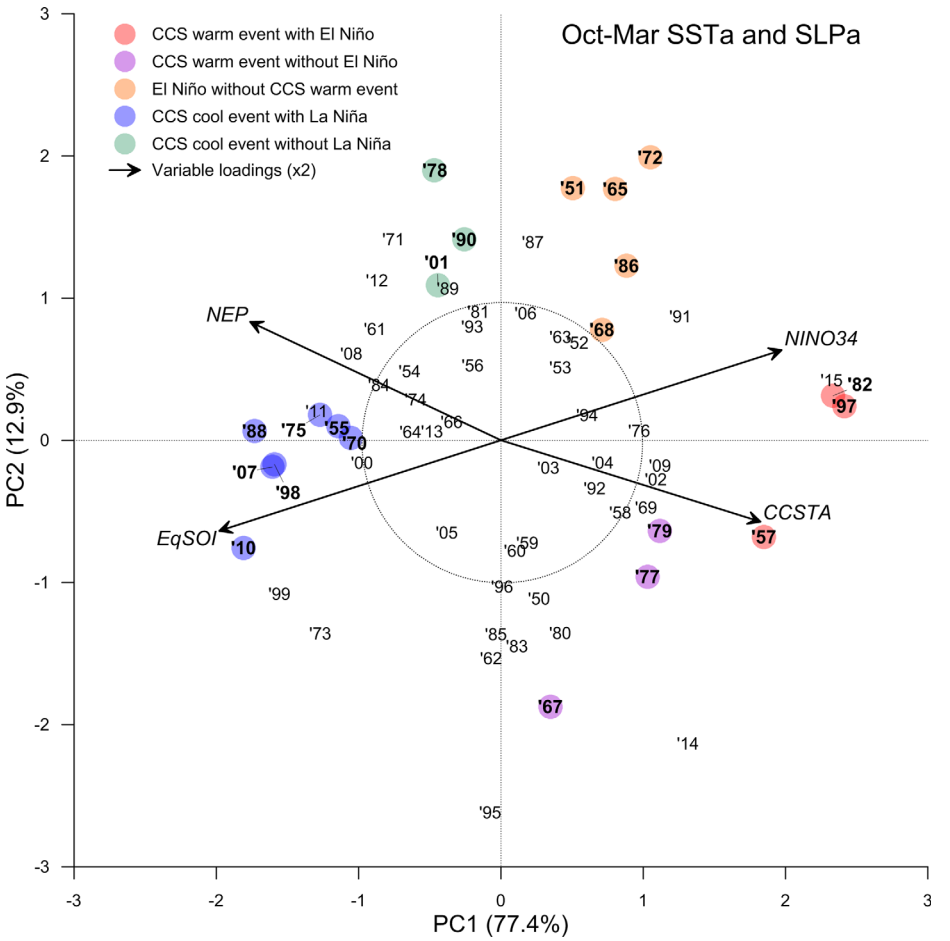

Figure 5. Ordination diagram for principal component analysis of surface temperature SSTa (CCSTA and NINO34) and atmospheric surface pressure SLPa (NEP and EqSOI) variables (standardized October–March means of 1950–2016 monthly data). Colors identify categories of warm/cool events selected as described in the text. The dotted circle marks standardized scores less than 1.

phase or uncorrelated. Winters with warm or cool events in only one region have more positive or negative scores on the vertical (PC2) axis.

Years selected for temporal and spatial composites in five regional warm/cool categories are identified in Figure 5:

1. CCS warm event with El Niño (1957, 1982, 1997),
2. CCS warm event without El Niño (1967, 1977, 1979),
3. El Niño without CCS warm event (1951, 1965, 1968, 1972, 1986),
4. CCS cool event with La Niña (1955, 1970, 1975, 1988, 1998, 2007, 2010), and
5. CCS cool event without La Niña (1978, 1990, 2001).

The sample size for three of the five composites is only 3 years. Using our criteria of standardized SSTa $>+1$ or <-1 for five or more consecutive months, no years could be assigned to a La Niña without CCS cool event category. As explained above, years that followed similar selected years were excluded (e.g., 1971, 1980, 1983, 1987, 2012); these were multiyear events. Some years were ambiguous, in the sense that they were not distinctly located in one category (Figure 1). For example in 1991, the CCS was cool during summer and then warmer in the subsequent winter; 1991 lies between groups of El Niño with and without a concurrent CCS warm event. 2008 was only weakly cool in both regions. In both 2002 and 2009, the CCS was warm but CCSTA was $<+1$. 1995 was a weak CCS warm event, but a weak tropical cool event (La Niña). The warm events of 2014–2016 will be discussed separately.

3.2. Warm Events

3.2.1. SST Variations

Temporal SSTa composites of California Current and tropical (El Niño) warm events, concurrent or not, are shown in Figure 6. In the composites, the October–March warm/cold events occur in the winter between years 0 and 1. The time series show considerable variability between individual events, but the composites illustrate consistent differences between categories of co-occurrence of CCS and El Niño warm events. Both events tend to peak during the winter between years 0 and 1. Many El Niños (5 out of 8 since 1950) occur without a CCS warm event. Half of CCS warm events (3 out of 6 since 1950) co-occur with an El Niño. The individual event plots show considerable variability among events. With the caveat that sample sizes are small, the composite CCS and tropical warm events are greater in amplitude when they co-occur than when they occur alone. The concurrent CCS warm event also tends to persist through the subsequent summer, after the El Niño has ended.

Spatial SSTa composites (Figure 7) also show that both CCS warm events and El Niños tend to be more pronounced when they co-occur than when they occur alone, as in the temporal composites (Figure 6). El Niños, either with or without a concurrent CCS warm event, tend to occur with negative SSTa in the central and eastern tropical Pacific and positive SSTa in the North Pacific during the preceding winter. When El Niño co-occurs with a CCS warm event, the composite shows a relatively narrow band of positive SSTa $>1^{\circ}$C along the West Coast of North America from Mexico to the Gulf of Alaska. For CCS warm events without a concurrent El Niño, no warming is seen in the North Pacific until the summer preceding the event,

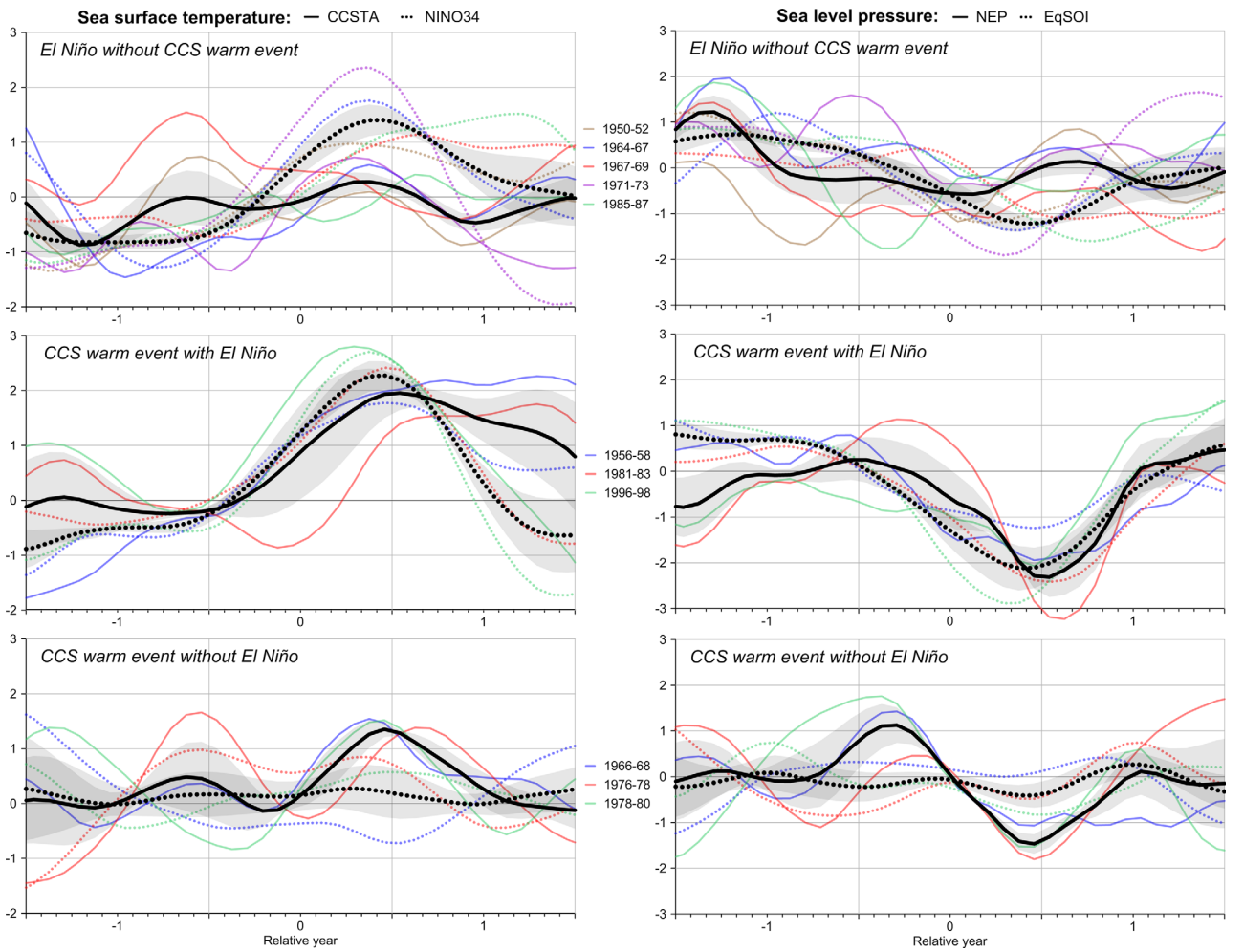

Figure 6. (left) Sea surface temperature: temporal composites of CCSTA and NINO34 standardized monthly SSTa for three categories of CCS warm events and/or tropical El Niños. (right) Atmospheric forcing: temporal composites of NEP and EqSOI standardized monthly SLPa for those categories. Colored lines are 12 month lowess smooths for individual events, heavy black lines are means ± standard error (sd × 2/n). Solid lines are CCS indices, dotted lines are tropical indices. Vertical grid lines are on the first day of January in years 0 and 1.

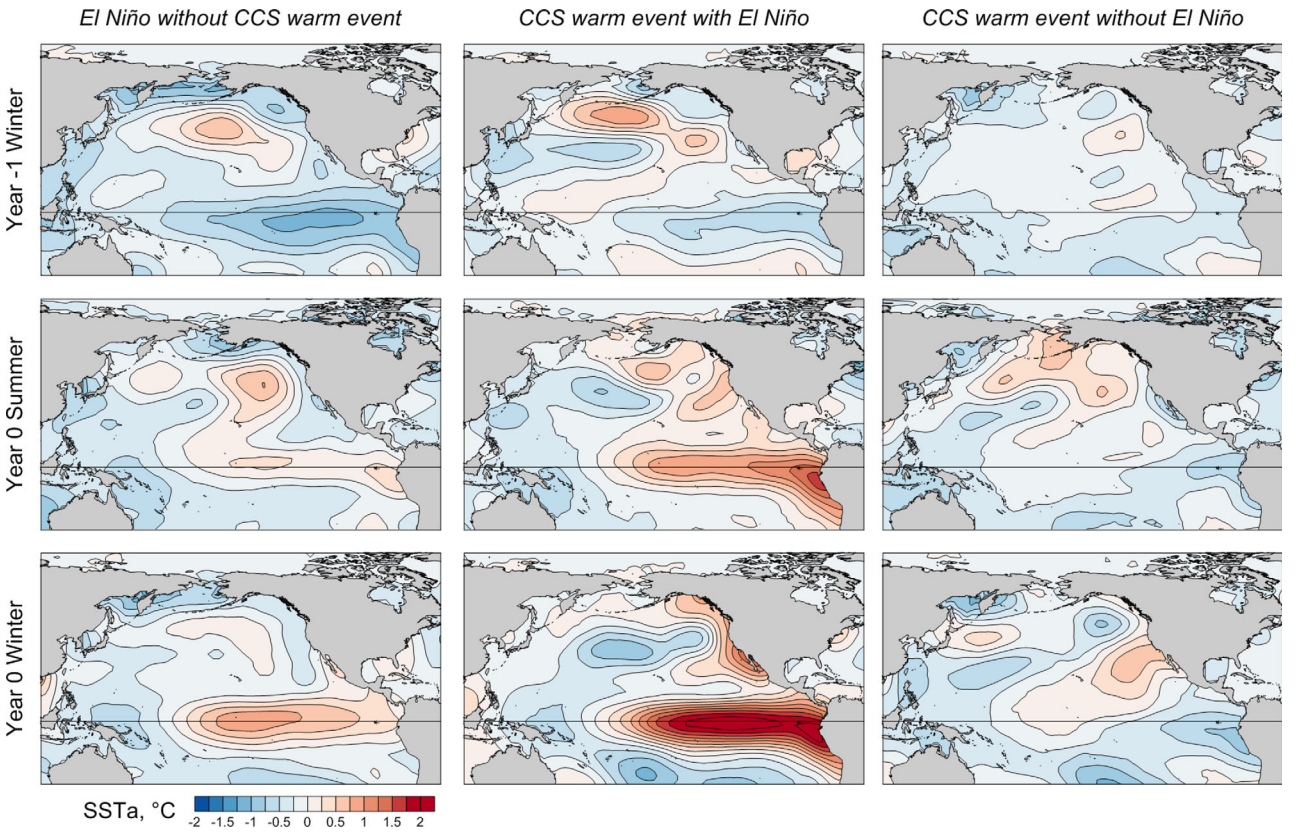

Figure 7. Sea surface temperature: spatial composites of 6-month means of monthly SSTa for El Niños and/or CCS warm events.

and the peak CCS warming in year 0 winter is part of a broad band extending from the West Coast toward Hawaii with relatively weak amplitude (<1°C).

3.2.2. Atmospheric Forcing

Spatial composites (Figure 8) show that the greatest SLP anomalies occur during winter to the south and east of the climatological position of the wintertime Aleutian Low pressure center; these variations are captured by the northeast Pacific SLPa index (NEP). Although SLPa values along the equator are less than in the North Pacific in these composites, the magnitude of wind vector anomalies is similar because of the latitudinal dependence of the Coriolis force and geostrophic wind balance. Temporal composites of NEP (Figure 6, right) show negative anomalies (intensification and southeastward displacement of the Aleutian Low) during winter when a CCS warm event occurs, with or without a concurrent El Niño. EqSOI is negative during an El Niño event, with or without a concurrent CCS warm event. A negative EqSOI indicates a reduced east-west SLP gradient and anomalously weak trade winds. As for NINO34, the composites indicate that when a CCS warm event occurs concurrently with an El Niño, the fluctuations in EqSOI are more pronounced.

The 6-month spatial composites of SLPa show these same patterns associated with CCS and tropical warm events, along with resulting surface wind anomalies (Figure 8). In winters preceding El Niño (year −1), the Aleutian Low is weak (positive SLPa). The weakening of the Aleutian Low is slightly greater when the California Current subsequently warms concurrently with the El Niño. CCS warm events without a concurrent El Niño are associated with a displacement of the Aleutian Low toward the west during the previous winter. The North Pacific winter positive SLP anomalies result in anticyclonic surface wind anomalies that represent a weakening of the normally strong temperate westerly winds at this time of year (Figure 2). There are no obvious changes in the equatorial SLPa gradient at this time, although trade winds in the eastern and central tropical Pacific are somewhat stronger.

During summer of the year when CCS and/or El Niño warm events peak (year 0), the North Pacific High weakens slightly. Coastal wind anomalies in much of the California Current region are poleward, indicating a weakening of the summer upwelling-favorable alongshore winds. There are only slight differences

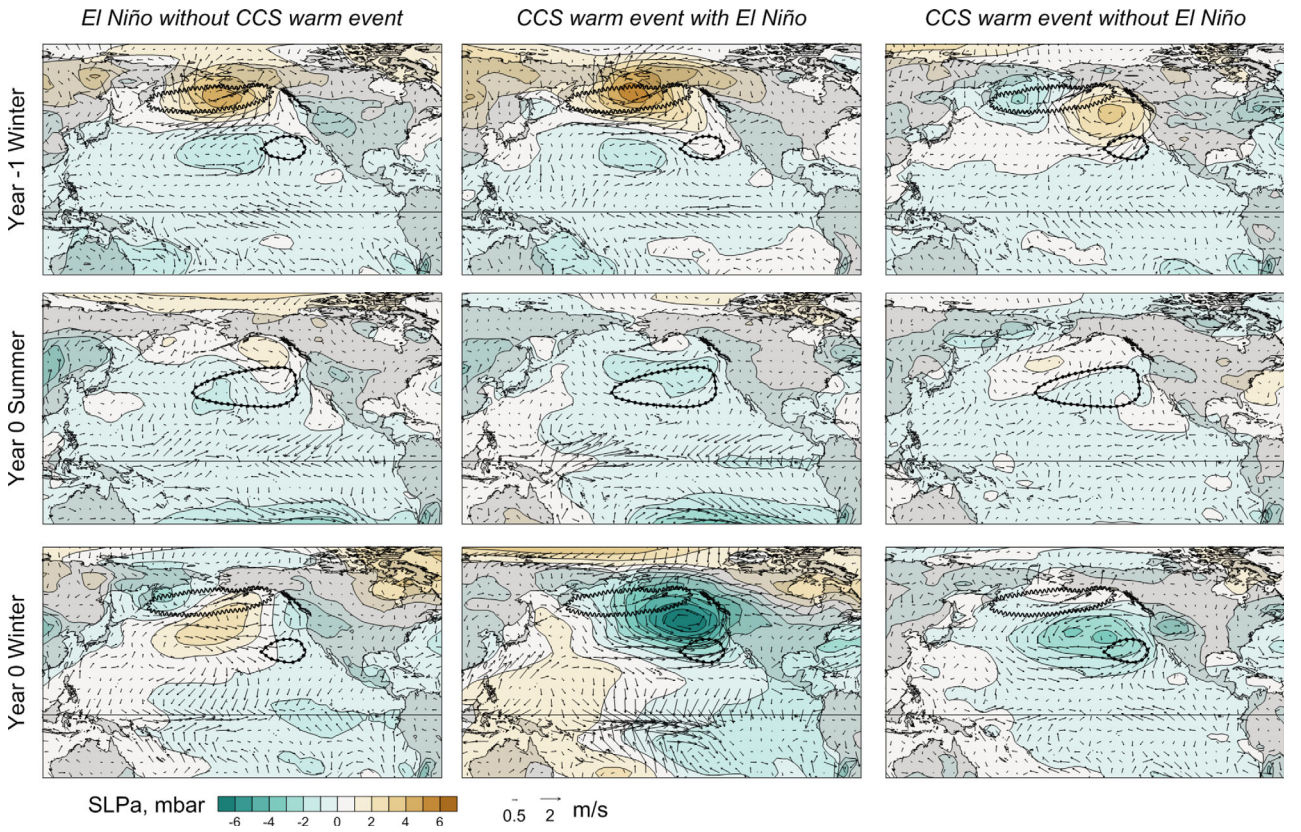

Figure 8. Atmospheric forcing: spatial composites of 6-month means of monthly SLPa and surface wind anomaly vectors for El Niños and/or CCS warm events. The climatological 1004 mb (wavy line) and 1020 mb (dotted line) isobars mark the climatological positions of the Aleutian Low and North Pacific High (Figure 2).

apparent in the summer coastal wind anomalies among the three categories of warm event co-occurrence. In the western tropical Pacific, westerly trade wind anomalies are seen in the El Niño composites, with or without a concurrent CCS warm event. The SLPa pattern in the summer "CCS warm event with El Niño" composite, where the trade wind anomalies are greatest, shows that the changes are associated with a weakening of the normal SLP gradient between the eastern and western tropical Pacific, i.e., a negative Southern Oscillation.

During winter when CCS warm events peak (year 0), SLPa is anomalously low in the northeast Pacific off the California coast and coastal wind anomalies are poleward, representing an intensification and southeastward displacement of the climatological wintertime Aleutian Low. This results in reduced coastal upwelling in the southern California Current region and increased downwelling to the north [*Jacox et al.*, 2014]. This pattern is much more pronounced when a concurrent El Niño occurs. When an El Niño is peaking without a CCS warm event, SLPa is slightly positive in much of the North Pacific to the south of the climatological Aleutian Low. The trade wind weakening during El Niño peaks in the central tropical Pacific during the winter of year 0. The SLPa pattern that results in a negative EqSOI anomaly is most apparent in the "CCS warm event with El Niño" composite: anomalously high SLP in the western tropical Pacific and low SLP in the eastern tropical Pacific.

3.3. Cool Events

3.3.1. SST Variations

No La Niña events without CCS cool events occurred during 1950–2015. Prior to 1950, however, such events occurred during the winters of 1924–1925, 1938–1939, and 1942–1943 (Figure 1). Most CCS cool events (7 out of 10 since 1950) co-occur with a La Niña (in comparison, 3 out of 6 CCS warm events co-occurred with an El Niño). The temporal composites for CCS cool events with or without La Niña (Figure 9) show that concurrent cool events tend to be very similar in both phase and magnitude, although the CCS cooling follows La Niña by 3–4 months. CCS cool events without La Niña tend to start later in the year (~October–

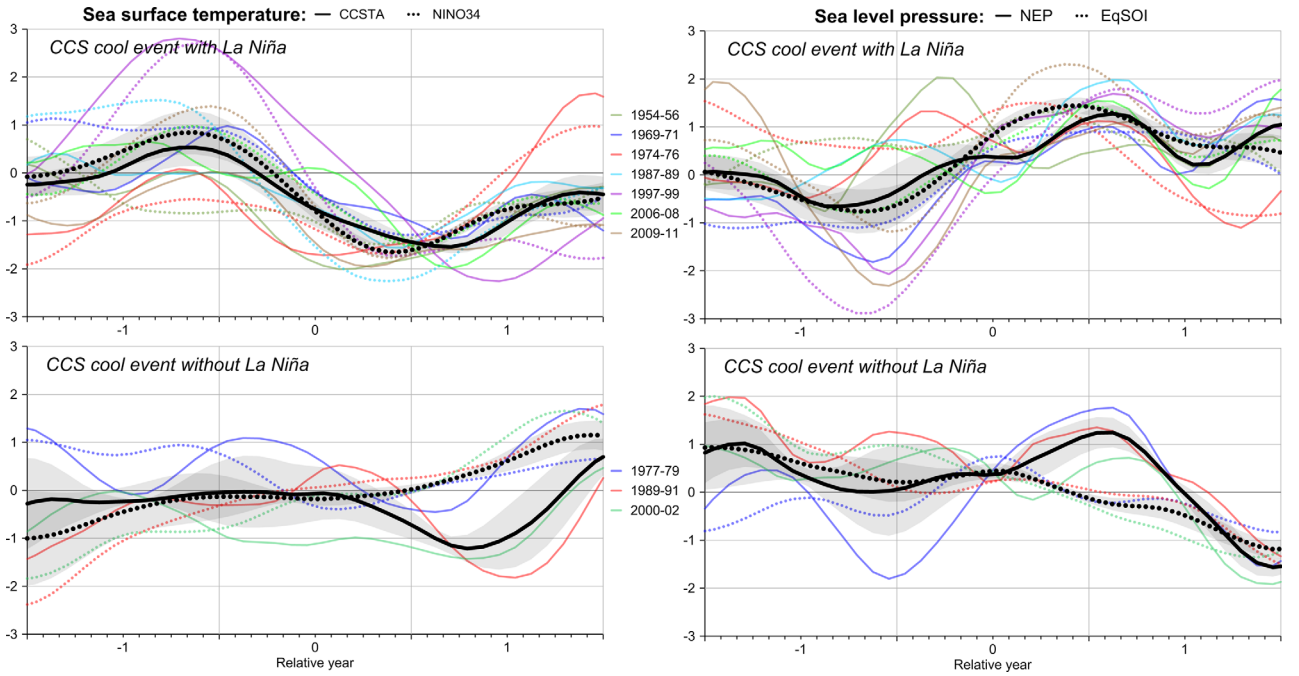

Figure 9. (left) Sea surface temperature: temporal composites of CCSTA and NINO34 standardized monthly SSTa for CCS cool events with or without a concurrent La Niña. (right) Atmospheric forcing: temporal composites of NEP and EqSOI standardized monthly SLPa for those categories. Colored lines are 12 month lowess smooths for individual events, heavy black lines are means ± standard error (sd × 2/n). Solid lines are CCS indices, dotted lines are tropical indices. Vertical grid lines are on the first day of January in years 0 and 1.

November) and peak later in late winter-early spring. As for warm events, CCS cool events are more intense when concurrent with a La Niña.

The spatial composites for concurrent cool events (Figure 10, left) are essentially the reverse of those for concurrent warm events (Figure 7, center), with the exception that La Niña SST anomalies in the eastern equatorial Pacific are less pronounced than are El Niño SST anomalies. In contrast, for CCS cool or warm events without a concurrent tropical event, there is no consistent relationship between the patterns of SST anomalies in the North Pacific outside of the CCS. CCS cool events tend to be more pronounced in the southern end of the system when there is a concurrent La Niña.

3.3.2. Atmospheric Forcing

Temporal composites of NEP (Figure 9, right) show positive anomalies (weak Aleutian Low) during winter when a CCS cool event occurs, with or without a concurrent La Niña. In contrast to warm events, the NEP anomaly tends to peak in winter at about +1.3 whether or not a concurrent La Niña event occurs. Also, EqSOI anomalies are positive during the La Niña, increasing during the previous summer. Spatial composites of SLPa and surface wind vectors during cool events (Figure 11) show an anomalously strong Aleutian Low during the winter prior to CCS cool events. This is opposite to the pattern for the preceding winter in CCS warm events (Figure 8). During the summer before CCS cool events, the North Pacific High is stronger than normal, but coastal winds in the CCS are anomalously equatorward only before CCS cool events with a concurrent La Niña. During winter of the CCS cool event, positive SLP anomalies in the North Pacific are associated with a weak or shifted Aleutian Low. The tropical anomalies preceding and during La Niña events in the left column of Figure 11 show the increased pressure gradient and trade winds in this phase of the ENSO cycle.

4. Discussion

We use correlation to infer likely causal relationships between potential forcing variables and SSTa. Although correlation is not sufficient evidence of causality, a statistically significant correlation between two variables is consistent either with a causal relationship or with a common forcing of the two. Cool-season (October–March) average SSTa in the California Current System (CCSTA) and in the central-eastern tropical Pacific (NINO34) are only modestly correlated at a level of 0.65. The corresponding regional SLPa indices

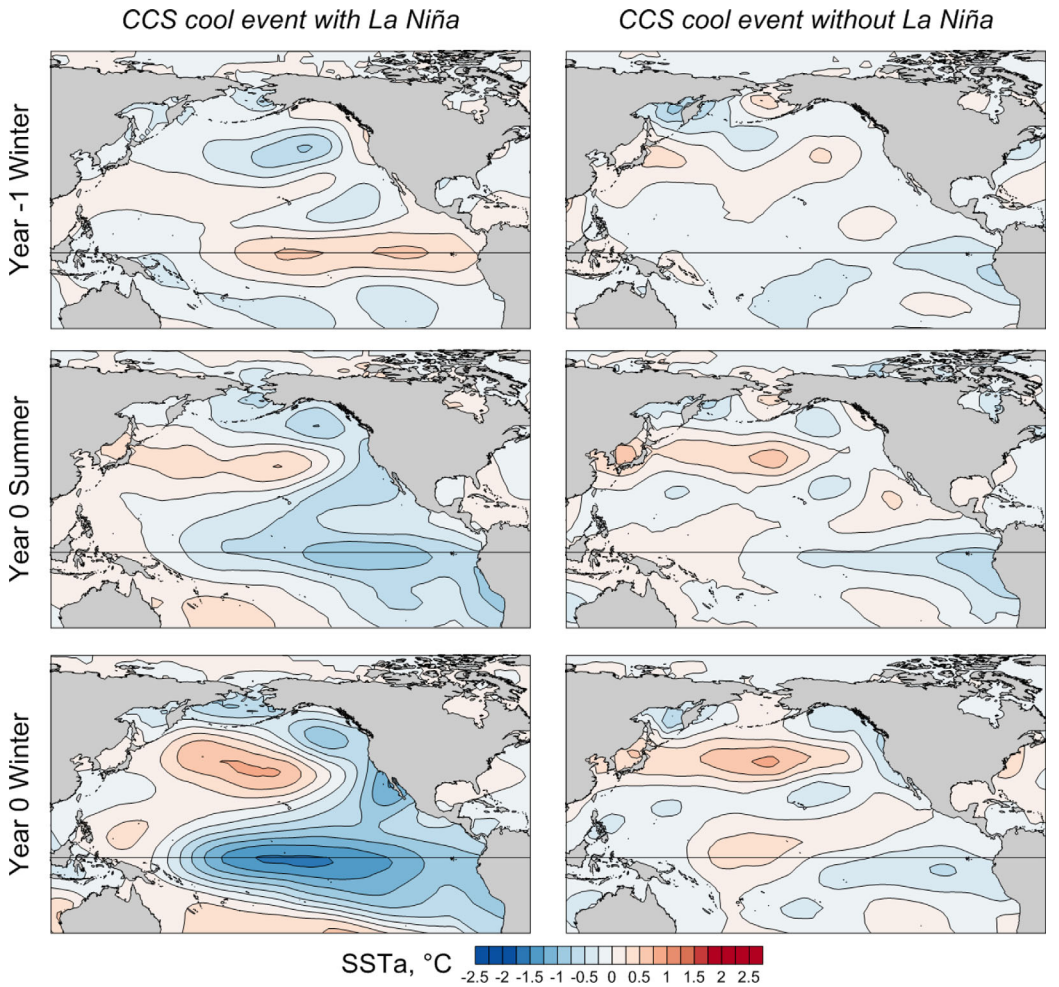

Figure 10. Sea surface temperature: spatial composites of 6-month means of monthly SSTa for CCS cool events with or without a concurrent La Niña.

represent atmospheric forcing by surface winds in the northeast (NEP) and tropical (EqSOI) Pacific. Correlations of these SLPa indices with the regional SSTa indices are consistent with atmospheric forcing of SST variations in the California Current related to SLP and surface wind variations in the northeast Pacific, but they also suggest a tropical influence. The spatial patterns of regression coefficients between the SLPa indices and the ERSST gridded time series of SSTa (Figure 4) are consistent with local forcing of interannual SSTa variability in the California Current by northeast Pacific atmospheric processes, but with a lesser influence of remote forcing from the tropics in the southern California Current. Warm/cold events do co-occur in the CCS and tropical Pacific regions; the enhancement of concurrent events seen in both the temporal and spatial composites highlights the importance of tropical/extratropical interactions in the extreme warm and cool years.

Our temporal and spatial composites of warm/cool events allow some conclusions about the effects of concurrent tropical events on CCS warm/cold events. Although the sample sizes for our composites are low (3–7), the differences between composites of categories of co-occurring events are consistent for individual events within categories. This can be seen both in the temporal composite plots of Figures 6 and 9, and in seasonal maps of individual events (not shown). Therefore, we are confident that the composites are representative of event types in the 1950–2016 period.

Our results are consistent with the known role of the Aleutian Low pressure system, and its teleconnection with the tropical Indo-Pacific, in the North Pacific. Variations in atmospheric pressure patterns associated with the Aleutian Low are known to drive interannual and decadal scale variability in the region [*Trenberth*

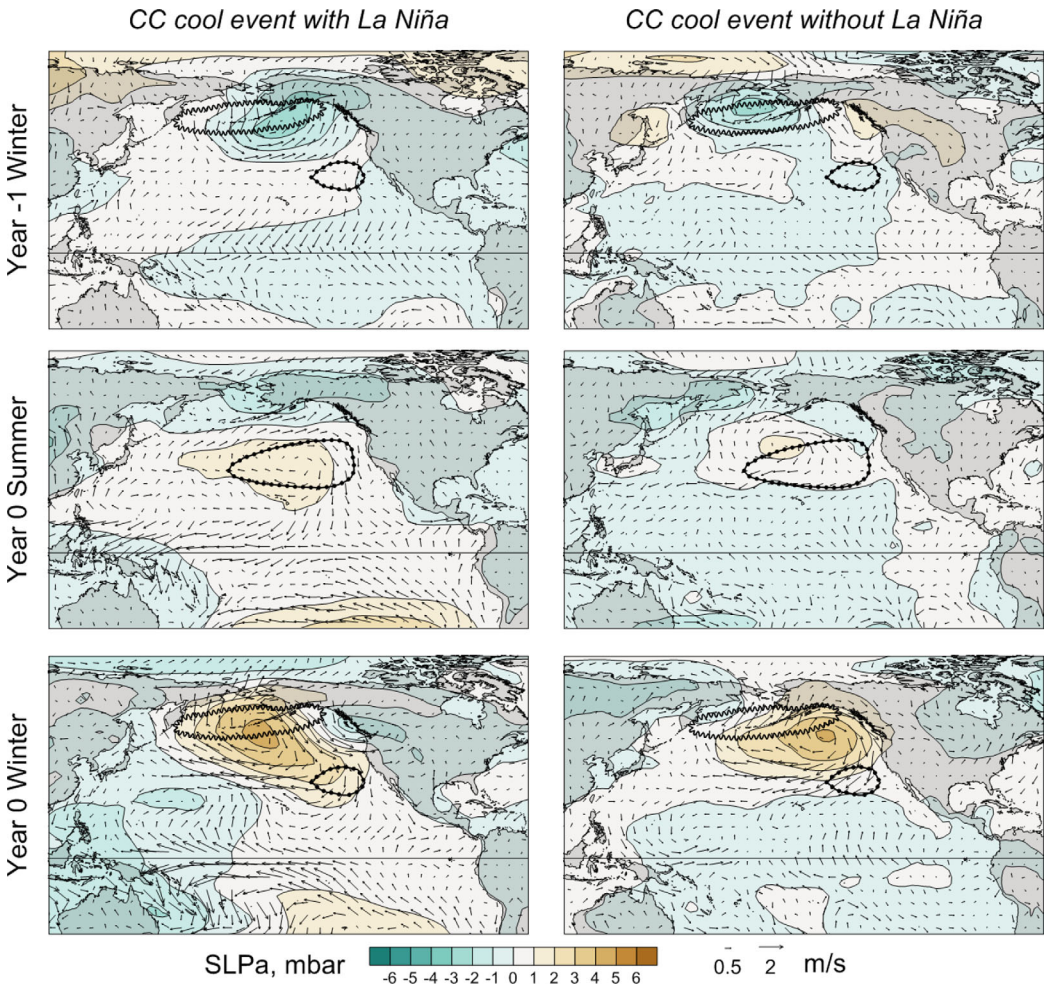

Figure 11. Atmospheric forcing: spatial composites of 6-month means of monthly SLPa and surface wind anomaly vectors for CCS cool events with or without a concurrent La Niña. The climatological 1004 mb (wavy line) and 1020 mb (dotted line) isobars mark the climatological positions of the Aleutian Low and North Pacific High (Figure 2).

and Hurrell, 1994; *Miller et al*., 2004; *Johnstone and Mantua*, 2014; *DiLorenzo and Mantua*, 2016]. *Emery and Hamilton* [1985] noted a relationship between ENSO and North Pacific pressure patterns, with a tendency for El Niño to concur with an intensified and southeastward displaced Aleutian Low, following winters with a weak or displaced Aleutian Low. We observed the same patterns, but only if the CCS warmed concurrently with a tropical El Niño (Figure 8). The weakening of the Aleutian Low during the preceding winter was less pronounced when the CCS warmed with no concurrent El Niño.

The temporal composites of warm events demonstrate that an intensified Aleutian Low, with associated weak equatorward winds along the US west coast, is a key factor for CCS warm event. Likewise, El Niño does not occur in the tropics without a weakening of the east-west SLP gradient and associated easterly trade winds. However, exceptional CCS warm events tend to co-occur with strong El Niño events. One interpretation of this observation is that the magnitude of the tropical/extratropical teleconnections linking ENSO to the CCS varies with the magnitude of the ENSO event, as do the effects of the teleconnections on the CCS [*Jacox et al*., 2015b]. Changes in the tropics can affect the North Pacific through an atmospheric teleconnection [*Alexander et al*., 2002] and upper-ocean processes that involve tropical-origin poleward propagating coastally trapped waves [*Enfield and Allen*, 1980, *Strub and James*, 2002; *Frischknecht et al*., 2015]. We found a correlation between NEP and EqSOI of +0.58, suggesting only a modest teleconnection between tropical and northeast Pacific SLP variations. During 1950–2013, 3 out of 6 CCS warm events occurred without an El Niño, 5 out of 8 El Niños occurred without a CCS warm event, and 3 out of 10 CCS cool events occurred without a tropical La Niña.

Following the major 1982–1983 El Niño and concurrent California Current warm event during winter 1982–1983 and summer 1983, *Simpson* [1984, 1992] demonstrated a tendency for the co-occurrence of California warm/cold events with strong El Niño/La Niñas, but with a smaller sample size available at that time. He argued that the CCS warm periods are associated with an expansion and intensification of the Aleutian Low, while the corresponding cold periods are associated with an expansion and intensification of the North Pacific High, and that this atmospheric forcing acted primarily through changes in onshore/offshore wind-driven transport, i.e., coastal upwelling. Our results support and extend Simpson's findings.

Variation in the CCS may also be driven by remote upper-ocean processes. Propagation of ENSO variability from the tropics was first discovered in coastal sea level records [*Enfield and Allen*, 1980]. During El Niño, trade wind anomalies produce equatorial Kelvin waves moving from west to east that, upon reaching the coast of South America, induce coastally trapped waves that move poleward along the Pacific coasts of North and South America. A recent model experiment showed that remote forcing—coastally trapped waves—dominates the interannual variability of SSH in the nearshore region of the CCS, but that local forcing, primarily wind-driven upwelling, tends to drive variations in SST throughout the CCS [*Frischknecht et al*., 2015]. These authors also found latitudinal variability in the relative importance of local and remote forcing for both physical and biogeochemical variables within the nearshore region. Our regression coefficient maps (Figure 4) suggest that local forcing is most important for CCS SST anomalies, except at the southern end off Baja California. *Yuan and Yamagata* [2014] demonstrated that interannual SST anomalies off Baja California, which they called California Niño/Niña, were related to local wind anomalies and even suggested that a local Bjerknes feedback could enhance these events.

We found that CCS warm events tend to persist into subsequent summers when they co-occur with an El Niño (Figure 6). *Jacox et al*. [2015b] demonstrated that not only are CCS coastal upwelling winds typically weak during El Niño winters, but source waters for upwelling are unusually shallow, warm, and fresh during the subsequent spring and summer. 2005 was a warm year in the northern California Current resulting from delayed summer upwelling [*Schwing et al*., 2006]. This summer warm event followed a moderate tropical El Niño (see Figure 1); however, neither event met the criteria for our analysis. As mentioned above, another unique year was 1995–1996 when both a weak CCS warm event and a weak tropical cool event (La Niña) occurred.

An even more extraordinary sequence of events began in the winter of 2013–2014, when the so-called North Pacific Blob first appeared [*Amaya et al*., 2016]. At this time, a high-pressure blocking ridge over the Gulf of Alaska resulted in very weak surface winds, which altered local heat exchange and resulted in extreme warm anomalies of the upper ocean [*Bond et al*., 2015]. Shortly thereafter, in early 2014, atmospheric changes in the tropics weakened trade winds and a significant El Niño was predicted for later in the year. A strong easterly wind burst in June 2014 stalled the development of the El Niño anticipated to mature in winter 2014–2015 [*Hu and Fedorov*, 2016], but also contributed to setting up a major El Niño in 2015–2016 [*Levine and McPhaden*, 2016]. During winter 2014–2015, the shape of the Blob changed and re-intensified, resulting in a multiyear marine heatwave that affected many components of regional marine ecosystems [*DiLorenzo and Mantua*, 2016]. These authors remark that this event was unprecedented, but may become more common as climate change increases the mean surface temperatures of the tropical and subtropical Pacific and intensifies thermodynamic ocean-atmosphere feedbacks.

Based on our criteria, 2014–2015 stands out as the most extreme warm event in the CCS without El Niño, while 2015–2016 was comparable to the co-occurring CCS/El Niño warm events in 1982–1983 and 1997–1998 (Figure 1). While we have focused on CCS warm and cold extremes at the scale of the entire West Coast, *Gentemann et al*. [2017] use satellite observations to show subregional scale features in the spatial-temporal evolution of the CCS warming from January 2014 to August 2016. Qualitatively speaking, the peak CCS warming in winter 2015 and winter 2016 resemble our composite winter CCS warm events without El Niño for their lack of amplified nearshore SST warm anomalies maximized along the West Coast, features of the 2015–2016 warming also noted by *Jacox et al*. [2016]. The 2015–2016 CCS warm period was also notable for having anomalously strong upwelling winds in the southern/central CCS, which is opposite to the typical pattern during El Niño periods [*Jacox et al*., 2016; *Frischknecht et al*., 2017]. Surprisingly, the CCS warming pattern from late summer 2014 into 2015, a period with tropical warming that failed to reach NOAA's criteria for declaring an El Niño event, showed more of the coastally amplified CCS warming featured in our

composites for events co-occurring with El Niño. *DiLorenzo and Mantua* [2015] attributed this to sustained ENSO-like regional atmospheric forcing in the northeast Pacific in fall 2014.

We chose to use SST as an indicator of CCS warm/cool events. SST represents mixed-layer temperature, which is directly influenced by ocean-atmosphere processes, but does not necessarily reflect changes in the thermocline or deeper waters. Our conclusions about the forcing of CCSTA variations and relationships with ENSO may need to be qualified by our choice of an indicator variable. *Norton and McLain* [1994] examined California Current warmings in the 0–300 m water column for 1954–1986, about half the length of our records. They found that CCS warmings that extended to depth were all associated with an El Niño, and that warming at 100–300 m was correlated at a 6-month lag with SLP changes in the western tropical Pacific while warming at the surface was more closely correlated with NE Pacific SLP changes. Thus, they concluded that CCS warmings concurrent with El Niño were remotely forced through the ocean at depth, but also locally forced by the atmosphere at the surface. Surface warming off California during El Niño is at least partly explained by a depressed pycnocline and change in deep source waters for coastal upwelling [*Jacox et al*., 2015b]. In contrast, the 2014 CCS warming was associated with local atmospheric forcing at the surface [*Zaba and Rudnick*, 2016].

Simpson [1992] emphasized that the changes in the California Current during the 1982–1983 warm event, with the concurrent tropical El Niño, comprised a broad range of variables in addition to SST: depression of the thermocline and increased sea levels along the coast, positive temperature and negative salinity anomalies at subsurface thermocline depths, positive dissolved oxygen and negative inshore nutrient anomalies. *Lluch-Belda et al*. [2003] analyzed variability in the California Current at three time scales—ENSO (5–7 years), bidecadal (20–30 years), and very low frequency (50–75 years)—and concluded that the system alternated between two opposing states at all of these scales. These states could be characterized as warm and cool, as in the present paper, but were shown to involve other physical variables and biological effects, specifically the advection of distinct planktonic communities. *Jacox et al*. [2017] explored predictability of California Current warm events with climate models, since this variability affects living marine resources with ecological and economic consequences. They also show that local wind forcing, influenced by tropical teleconnection, drives ENSO-related variability in the CCS in ways that contribute to increased predictability of seasonal SST variations.

Unusually warm or cold surface waters in the California Current can result from changes in the magnitude, phenology, or source-water characteristics of both upwelling and advection processes. Weak and delayed summer upwelling in 2005 impacted seabirds and rockfish off central California and zooplankton off Oregon [*Schwing et al*., 2006]. The 1997–1999 ENSO cycle, and the concurrent CCS warm and cool events, had pervasive ecosystem effects including the physical structure and circulation dynamics [*Lynn and Bograd*, 2002], nutrient availability and primary production [*Chavez et al*., 2002], zooplankton production [*Bograd and Lynn*, 2001], and cetacean community composition and prey availability [*Benson et al*., 2002]. Other CCS warm events, with or without associated tropical El Niños, have been shown to affect zooplankton community structure [*Fisher et al*., 2015], and the prey resources and juvenile survival of California sea lions [*Weise and Harvey*, 2008; *McClatchie et al*., 2016]. We found that the magnitude and persistence of warm/cold events in this ecosystem are related to concurrent ENSO events; it is important to understand the linkage between the tropical Pacific and the California Current in forecasting ecosystem variations in the future [*Ohman et al*., 2017].

5. Conclusions

Contrary to conventional wisdom, there is only a modest correlation between interannual extremes in tropical ENSO and California Current System SST variations ($r^2 = 42\%$). Local atmospheric forcing can explain most of the interannual variability in CCS SST variations from 1950 to 2013, but the teleconnection between tropical ENSO variations and local atmospheric forcing is weak ($r^2 = 34\%$). The strongest ENSO and CCS SST extremes are observed when they are co-occurring. The correspondence between tropical La Niña and cold events in the CCS is more robust than that between El Niño and warm events in the CCS.

Year-to-year changes in the CCS must be viewed in the context of both regional and remote forcing. ENSO-related remote forcing via tropical trade winds and equatorial Kelvin waves are best correlated with SST variations in the extreme southern part of the CCS; however, these correlations probably reflect a mix of local

atmospheric forcing (surface heat flux and Ekman transports) that is coherent with the Southern Oscillation, and poleward propagating coastally trapped waves that are also driven by variations in the Southern Oscillation (via equatorial wave dynamics).

Acknowledgments
No external funding sources were used in this work. All data are available from the sources specified in the text. We thank Sam McClatchie and Michael Jacox for comments on an early version. Two anonymous reviewers have greatly improved the paper.

References

Alexander, M., I. Blade, M. Newman, J. Lanzante, N. Lau, and J. Scott (2002), The atmospheric bridge: The influence of ENSO teleconnections on air-sea interaction over the global oceans, *J. Clim.*, *15*(16), 2205–2231, doi:10.1175/1520-0442(2002)0152.0.CO;2.

Amaya, D. J., N. E. Bond, A. J. Miller, and M. J. DeFlorio (2016), The evolution and known atmospheric forcing mechanisms behind the 2013–2015 North Pacific warm anomalies, *U.S. CLIVAR Variations*, *14*(2), 1–6.

Benson, S. R., D. A. Croll, B. B. Marinovic, F. P. Chavez, and J. T. Harvey (2002), Changes in the cetacean assemblage of a coastal upwelling ecosystem during El Niño 199798 and La Niña 1999, *Prog. Oceanogr.*, *54*, 279–291.

Bjerknes, J. (1969), Atmospheric teleconnections from the equatorial Pacific, *Mon. Weather Rev.*, *97*, 163–172.

Bograd, S. J., and R. J. Lynn (2001), Physical-biological coupling in the California Current during the 1997–99 El Niño-La Niña cycle, *Geophys. Res. Lett.*, *28*, 275–278.

Bond, N. A., M. F. Cronin, H. Freeland, and N. J. Mantua (2015), Causes and impacts of the 2014 warm anomaly in the NE Pacific, *Geophys. Res. Lett.*, *42*, 3414–3420, doi:10.1002/2015GL063306.

Chavez, F. P., J. T. Pennington, C. G. Castro, J. P. Ryan, R. P. Michisaki, B. Schlining, P. Walz, K. R. Buck, A. McFadyen, and C. A. Collins (2002), Biological and chemical consequences of the 1997–1998 El Niño in central California waters, *Prog. Oceanogr.*, *54*, 205–232.

Deser, C., M. A. Alexander, S.-P. Xie, and A. S. Phillips (2010), Sea surface temperature variability: Patterns and mechanisms, *Annu. Rev. Mar. Sci.*, *2*, 115–143.

DiLorenzo, E., and N. Mantua (2016), Multi-year persistence of the 2014/15 North Pacific marine heatwave, *Nat. Clim. Change*, *6*(11), 1042–1047, doi:10.1038/NCLIMATE3082.

Emery, W. J., and K. Hamilton (1985), Atmospheric forcing of interannual variability in the northeast Pacific Ocean: Connections with El Niño, *J. Geophys. Res.*, *90*, 857–868.

Enfield, D., and J. Allen (1980), On the structure and dynamics of monthly mean sea-level anomalies along the Pacific coast of North and South America, *J. Phys. Oceanogr.*, *10*(4), 557–578.

Fisher, J. L., W. T. Peterson, and R. R. Rykaczewski (2015), The impact of El Niño events on the pelagic food chain in the northern California Current, *Global Change Biol.*, *21*, 4401–4414.

Frischknecht, M., M. Münnich, and N. Gruber (2015), Remote versus local influence of ENSO on the California Current System, *J. Geophys. Res.*, *120*, 1353–1374, doi:10.1002/2014JC010531.

Frischknecht, M., M. Münnich, and N. Gruber (2017), Local atmospheric forcing driving an unexpected California Current System response during the 2015–2016 El Niño, *Geophys. Res. Lett.*, *44*, 304–311, doi:10.1002/2016GL071316.

Gentemann, C. L., M. R. Fewings, and M. García-Reyes (2017), Satellite sea surface temperatures along the West Coast of the United States during the 2014–2016 northeast Pacific marine heat wave, *Geophys. Res. Lett.*, *44*, 312–319, doi:10.1002/2016GL071039.

Hobday, A. J., et al. (2016), A hierarchical approach to defining marine heatwaves, *Prog. Oceanogr.*, *141*, 227–238.

Hu, S., and A. V. Fedorov (2016), Exceptionally strong easterly wind burst stalling El Niño of 2014, *Proc. Natl. Acad. Sci. U. S. A.*, *113*(8), 2005–2010.

Huang, B., V. F. Banzon, E. Freeman, J. Lawrimore, W. Liu, T. C. Peterson, T. M. Smith, P. W. Thorne, S. D. Woodruff, and H.-M. Zhang (2015), *Extended Reconstructed Sea Surface Temperature (ERSST), Version 4*, NOAA Natl. Cent. for Environ. Inf., doi:10.7289/V5KD1VVF. [Available at https://www.ncdc.noaa.gov/data-access/marineocean-data/extended-reconstructed-sea-surface-temperature-ersst-v4.]

Jacox, M. G., et al. (2014), Spatially resolved upwelling in the California Current System and its connections to climate variability, *Geophys. Res. Lett.*, *41*, 3189–3196, doi:10.1002/2014GL059589.

Jacox, M. G., S. J. Bograd, E. L. Hazen, and J. Fiechter (2015a), Sensitivity of the California Current nutrient supply to wind, heat, and remote ocean forcing, *Geophys. Res. Lett.*, *42*, 5950–5957, doi:10.1002/2015GL065147.

Jacox, M. G., J. Fiechter, A. M. Moore, and C. A. Edwards (2015b), ENSO and the California Current coastal upwelling response, *J. Geophys. Res.*, *120*, 1691–1702, doi:10.1002/2014JC010650.

Jacox, M. G., E. L. Hazen, K. D. Zaba, D. L. Rudnick, C. A. Edwards, A. M. Moore, and S. J. Bograd (2016), Impacts of the 2015–2016 El Niño on the California Current System: Early assessment and comparison to past events, *Geophys. Res. Lett.*, *43*, 7072–7080, doi:10.1002/2016GL069716.

Jacox, M. G., M. A. Alexander, C. A. Stock, and G. Hervieux (2017), On the skill of seasonal sea surface temperature forecasts in the California Current System and its connection to ENSO variability, *Clim. Dyn.*, 1–15, doi:10.1007/s00382-017-3608-y.

Johnstone, J. A., and N. J. Mantua (2014), Atmospheric controls on northeast Pacific temperature variability and change, 1900–2012, *Proc. Natl. Acad. Sci. U. S. A.*, *111*(40), 14,360–14,365, doi:10.1073/pnas.1318371111.

Kistler, R., et al. (2001), The NCEP-NCAR 50-rear reanalysis: Monthly means CD-ROM and documentation, *Bull. Am. Meteorol. Soc.*, *82*, 247–267.

Levine, A. F. Z., and M. J. McPhaden (2016), How the July 2014 easterly wind burst gave the 2015–2016 El Niño a head start, *Geophys. Res. Lett.*, *43*, 6503–6510, doi:10.1002/2016GL069204.

Li, B., and A. J. Clarke (1994), An examination of some ENSO mechanisms using interannual sea level at the eastern and western equatorial boundaries and the zonally averaged equatorial wind, *J. Phys. Oceanogr.*, *24*, 681–690.

Liu, Z., and M. A. Alexander (2007), Atmospheric bridge, oceanic tunnel and global climatic teleconnections, *Rev. Geophys.*, *45*, RG2005, doi:10.1029/2005RG000172.

Lluch-Belda, D., D. B. Lluch-Cota, and S. E. Lluch-Cota (2003), Scales of interannual variability in the California current system: Associated physical mechanisms and likely ecological impacts, *CalCOFI Rep.*, *44*, 76–85.

Lynn, R. J., and S. J. Bograd (2002), Dynamic evolution of the 1997–1999 El Niño-La Niña cycle in the southern California Current System, *Prog. Oceanogr.*, *54*, 59–75.

McClatchie, S., J. Field, A. R. Thompson, T. Gerrodette, M. Lowry, P. C. Fiedler, W. Watson, K. Nieto, and R. D. Vetter (2016), Food limitation of sea lion pups and the decline of forage off central and southern California, *R. Soc. Open Sci.*, *3*, 150,628.

McPhaden, M. J., S. E. Zebiak, and M. H. Glantz (2006), ENSO as an integrating concept in earth science, *Science*, *314*, 1740–1745.

Miller, A. J., F. Chai, S. Chiba, J. R. Moisan, and D. J. Neilson (2004), Decadal-scale climate and ecosystem interactions in the North Pacific Ocean, *J. Oceanogr.*, *60*, 163–188.

Mysak, L. A. (1986), El Niño, interannual variability and fisheries in the northeast Pacific Ocean, *Can. J. Fish. Aquat. Sci.*, *43*, 464–497.
Norton, J. G., and D. R. McLain (1994), Diagnostic patterns of seasonal and interannual temperature variation off the west coast of the United States: Local and remote large-scale atmospheric forcing, *J. Geophys. Res.*, *99*, 16,019–16,030.
Ohman, M. D., N. Mantua, J. Keister, M. Garcia-Reyes, and S. McClatchie (2017), ENSO impacts on ecosystem indicators in the California Current System, *U.S. CLIVAR Variations*, *15*(1), 8–15.
Scannell, H. A., A. J. Pershing, M. A. Alexander, A. C. Thomas, and K. E. Mills (2016), Frequency of marine heatwaves in the North Atlantic and North Pacific since 1950, *Geophys. Res. Lett.*, *43*, 2069–2076, doi:10.1002/2015GL067308.
Schwing, F. B., N. A. Bond, S. J. Bograd, T. Mitchell, M. A. Alexander, and N. Mantua (2006), Delayed coastal upwelling along the U.S. West Coast in 2005: A historical perspective, *Geophys. Res. Lett.*, *33*, L22S01, doi:10.1029/2006GL026911.
Sette, O. E., and J. D. Isaacs (Eds.) (1960), Symposium on "The changing Pacific Ocean in 1957 and 1958", *CalCOFI Rep.*, *7*, 13–217.
Simpson, J. J. (1984), Warm and cold episodes in the California Current: A case for large-scale mid-latitude atmospheric forcing, in *Proceedings of the Ninth Annual Climate Diagnostics Workshop, Oct. 22–26, 1984*, Corvallis, Oregon. Natl. Oceanic and Atmos. Admin, U. S. Dep. of Comm., pp. 173–184. [Available at https://www.ncdc.noaa.gov/data-access/marineocean-data/extended-reconstructed-sea-surface-temperature-ersst-v4.]
Simpson, J. J. (1992), Response of the Southern California current system to the mid-latitude North Pacific coastal warming events of 1982–1983 and 1940–1941, *Fish. Oceanogr.*, *1*(1), 57–79.
Strub, P. T., and C. James (2002), The 1997–1998 oceanic El Niño signal along the southeast and northeast Pacific boundaries—An altimetric view, *Prog. Oceanogr.*, *54*(1–4), 439–458, doi:10.1016/S0079-6611(02)00063-0.
Trenberth, K. E. (1997), The definition of El Niño, *Bull. Am. Meteorol. Soc.*, *78*(12), 2771–2777.
Trenberth, K. E., and J. W. Hurrell (1994), Decadal atmosphere–ocean variations in the Pacific, *Clim. Dyn.*, *9*, 303–319.
Weise, M. J., and J. T. Harvey (2008), Temporal variability in ocean climate and California sea lion diet and biomass consumption: Implications for fisheries management, *Mar. Ecol. Prog. Ser.*, *373*, 157–172.
Yuan, C., and T. Yamagata (2014), California Niño/Niña, *Sci. Rep.*, *4*, 4801, doi:10.1038/srep04801.
Zaba, K. D., and D. L. Rudnick (2016), The 2014–2015 warming anomaly in the Southern California Current System observed by underwater gliders, *Geophys. Res. Lett.*, *43*, 1241–1248, doi:10.1002/2015GL067550.